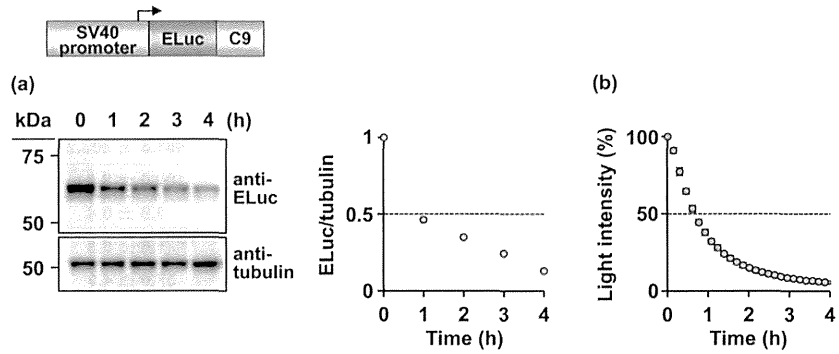

Fig. 3. Rapid decay of protein amount and activity of CAPN3-C9-fused ELuc in NIH3T3 cells. Expression plasmid SV40-ELuc::CAPN3-C9 was transfected into NIH3T3 cells. One day after transfection, the medium was replaced with DMEM supplemented with 10% FBS, 200 μM D-luciferin, and 100 μM cycloheximide. (a) Western blot analysis (left panel) and quantified data (right panel) of CAPN3-C9-fused ELuc. The transfected cells were harvested 0, 1, 2, 3, and 4 h after the medium change. Luciferase was detected using anti-ELuc antibody. Tubulin was used as the internal control. The positions of molecular weight markers are indicated on the left of the panel. To quantify the change in protein amount, the intensity of the bands for ELuc was normalized to that for tubulin, and time 0 was set to 1. (b) Functional half-life of CAPN3-C9-fused ELuc (also shown in Fig. S4). Schematic drawing of the plasmid is shown at the top.

(Fig. 5). NF-κB exists in an inactive form in the cytoplasm due to its interaction with IκB. After activation of the IκB kinase by TNFα, IκB is phosphorylated, ubiquitinated, and degraded. The dissociated NF-κB becomes free to translocate to the nucleus where it acutely activates specific target genes through selective binding to the NF-κB response element (Ling and Kumar, 2012).

To verify the effects of destabilization sequences on the sensitivity of the luciferase reporter assay using unmodified or destabilized ELuc, we inserted reporter plasmids into a multi-integrase human artificial chromosome (MI-HAC) vector (Yamaguchi et al., 2011) (Fig. 5a), which was generated by deleting all of the endogenous genes of human chromosome 21, and was stably maintained as a single copy in the host cells (Katoh et al., 2004; Kazuki et al., 2011).

Reporter plasmids carrying unmodified or destabilized ELuc under control of six tandem repeats of the NF-κB response element and the TK promoter were inserted into the φC31 attB site of the MI-HAC vector in mouse fibroblast A9 cells, in which the expression cassette was flanked by a tandem repeat of the HS4 insulator to prevent promoter interference (Fig. 5a). The site-specific insertion of the reporter plasmids into the MI-HAC vector was verified by genomic PCR (Fig. S6a) and FISH analysis (Fig. 5b). In the FISH analysis, signals from biotin-labeled reporter plasmids (green) were observed only on the MI-HAC vector that was labeled with digoxigenin (red), and not on the chromosome stained with DAPI (blue). Then, we examined again the half-lives of unmodified, PEST-fused, and C9-fused ELuc. Those luciferases were inserted into the MI-HAC vector in A9 cells (Fig. S6b). Consistent with their half-lives in NIH3T3 cells (Fig. 2a), we confirmed that C9-fused ELuc displayed the shortest half-life (0.43 h) compared with unmodified ELuc (5.90 h) and PEST-fused ELuc (1.48 h). The half-lives of all the luciferases in A9 cells were approximately half of those in NIH3T3 cells in which luciferase genes were introduced by transient transfection. We assume that those differences are due to differences in the plasmid copy number and the amount of luciferase expressed in the cells, because one copy of the luciferase gene is kept in the MI-HAC vector in A9 cells, whereas it was maintained at a high copy number in NIH3T3 cells.

The A9 stable cell lines carrying the NF-κB reporter plasmid on the MI-HAC vector were transiently treated with TNFα for 15 min, and bioluminescence was recorded in real time. The

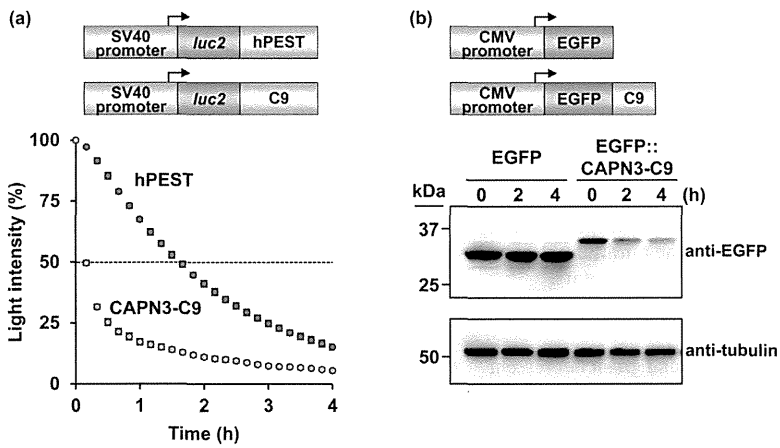

Fig. 4. Destabilization of firefly luciferase (*luc2*) and EGFP by C9 fragment in NIH3T3 cells. (a) Stability of hPEST-fused *luc2*, and CAPN3-C9-fused *luc2* in NIH3T3 cells. Expression plasmid pSV40-luc2::hPEST or pSV40-luc2::CAPN3-C9 was transfected into NIH3T3 cells seeded in 96-well plates. One day after transfection, the culture medium was replaced with DMEM supplemented with 10% FBS, 200 μM D-luciferin, and 100 μM cycloheximide. Bioluminescence was recorded in real time for 10 s at 10-min intervals for 4 h at 37 °C. The maximum peak values were set to 100%. Error bars indicate the standard deviation ($n = 6$). (b) Western blot analysis of unmodified EGFP and CAPN3-C9-fused EGFP in NIH3T3 cells. The expression plasmid pEFGP-C2 or pCMV-EGFP::CAPN3-C9 was transfected into NIH3T3 cells, and incubation was carried out for two days. The culture medium was replaced with DMEM supplemented with 10% FBS and 100 μM cycloheximide, and incubation was carried out for 0, 2, and 4 h. EGFP was detected using the anti-EGFP antibody. Tubulin was used as the internal control. The positions of the molecular weight markers are indicated on the left of each panel. Schematic drawings of the plasmids are shown at the top.

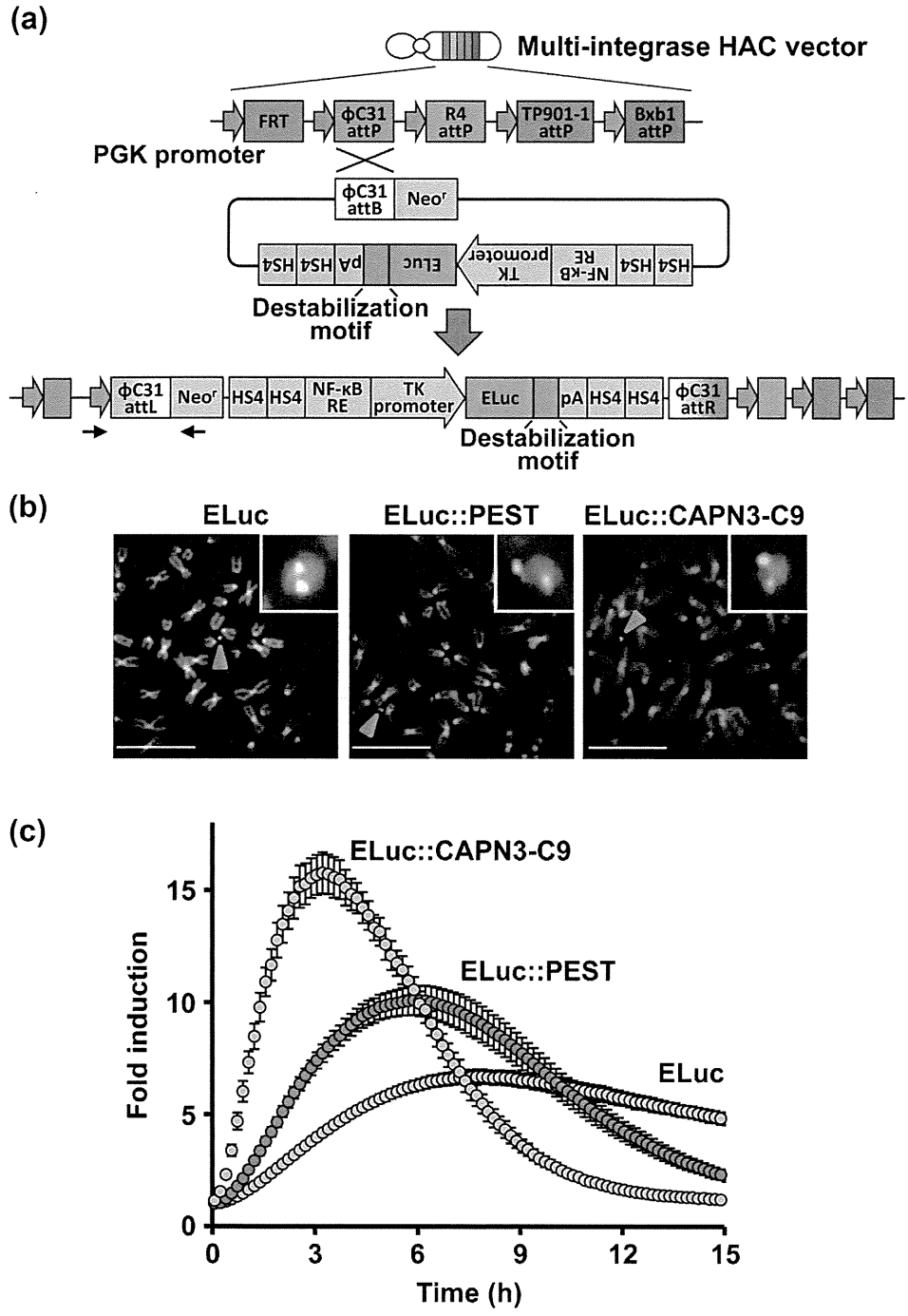

Fig. 5. Real-time bioluminescence recording of TNFα-induced transactivation of NF-κB with destabilized ELuc in A9 cells harboring the MI-HAC vector. (a) Schematic diagram of the site-specific insertion of the NF-κB reporter plasmid into the MI-HAC vector. Schematic diagrams of the MI-HAC vector and the multi-integrase platform are shown on top. NF-κB reporter plasmid was inserted into the φC31 attP site of the MI-HAC vector by φC31 recombinase-mediated homologous recombination in A9 cells. Neo^r, HS4, and NF-κB represent neomycin resistance gene, HS4 insulator, and six tandem repeats of the NF-κB response element, respectively. Arrowheads indicate primers used for genomic PCR to verify insertion of the reporter plasmid into the MI-HAC vector. (b) FISH analysis of A9 cells harboring the MI-HAC vector into which NFκB-ELuc (left panel), NFκB-ELuc::PEST (middle panel), and NFκB-ELuc::CAPN3-C9 (right panel) reporter plasmids were inserted. The A9 cells during metaphase were probed with digoxigenin-labeled human COT-1 (red) that hybridized with the HAC vector, and the biotin-labeled NF-κB reporter plasmid (green). Arrowheads indicate the HAC vector, and insets show enlarged images. Chromosome DNA was counter-stained with DAPI (scale bar, 10 μm). (c) Real-time bioluminescence recording of TNFα-induced transactivation of NF-κB, monitored by unmodified ELuc (green circles), PEST-fused ELuc (blue circles), and CAPN3-C9-fused ELuc (orange circles). The A9 cells harboring the MI-HAC vector into which the NF-κB reporter plasmid was integrated were seeded in 35-mm dishes, and treated with 10 ng/ml TNFα for 15 min. Then, the medium was replaced with DMEM without phenol red supplemented with 10% FBS and 200 μM D-luciferin. Bioluminescence was recorded in real time for 1 min at 10-min intervals for 15 h. Counts of TNFα-treated cells were divided by that of untreated cells, and the initial values (time = 0) were set to 1. Error bars indicate standard deviation ($n = 4$).

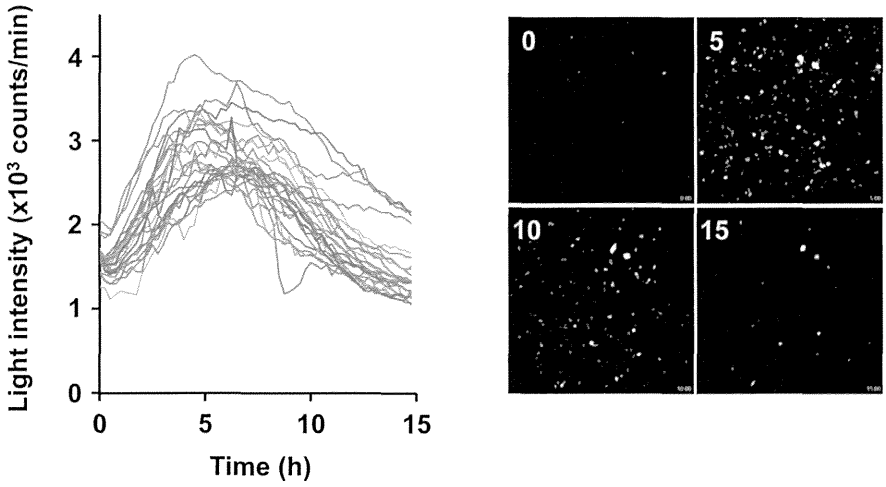

Fig. 6. Time-lapse bioluminescence imaging of TNFα-induced transactivation of NF-κB in A9 cells using CAPN3-C9-fused ELuc. A9 cells harboring the MI-HAC vector into which the NF-κB-ELuc::CAPN3-C9 reporter plasmid was integrated were seeded in 35-mm glass-bottom dishes, and treated with 10 ng/ml TNFα for 15 min. Then, the medium was replaced with DMEM supplemented with 10% FBS and 500 μM D-luciferin. CCD images were acquired with a 10-min exposure time at 15-min intervals for 15 h with a 4× objective lens. Recordings of luminescence from 25 cells and serial CCD images at 5-h intervals are shown on left and right panels, respectively.

time-dependent change of NF-κB activation was expressed as fold induction where bioluminescence intensity of the TNFα-treated cells was normalized to that of the TNFα-untreated cells at each time point. As shown in Fig. 5c, the NF-κB activation by TNFα monitored by unmodified ELuc was slowly increased and reached a maximum (6.69 ± 0.32-fold, mean ± SD) at 7.68 ± 0.10 h. This was followed by a very slow decay owing to residual luciferase protein in the cells (green circles). The fold induction and the peak time monitored by PEST-fused ELuc were 10.01 ± 0.66-fold and 5.11 ± 0.22 h, respectively (blue circles), indicating more sensitive monitoring of the activation than the unmodified ELuc. As expected, the most rapid activation and the subsequent rapid decay of bioluminescence could be monitored by using ELuc fused to the CAPN3 C9 fragment, and the fold induction and the peak time were 15.78 ± 0.92-fold and 3.47 ± 0.18 h, respectively (orange circles). Although the light intensity of C9-fused ELuc was 1.0% of that of PEST-fused ELuc (Fig. S6c), we were able to reliably quantify the activation kinetics of NF-κB, demonstrating that the C9 fragment is a suitable destabilization sequence for monitoring gene expression. Our results indicate that the CAPN3 C9 fragment identified in this study acts as rapid degradation signal compared with the PEST sequence of ornithine decarboxylase, enabling highly sensitive monitoring of cellular response using the luciferase reporter gene.

3.5. Time-lapse single-cell bioluminescence imaging using CAPN3-C9-fused ELuc

Recent advances in luciferase technology have enabled the quantitative visualization of gene expression at single-cell resolution by monitoring luminescence in real time using a highly sensitive CCD camera (Nakajima et al., 2010; Roda et al., 2009; Welsh et al., 2010). Although fluorescence imaging techniques that use fluorescent proteins as probes have contributed immensely to the advancement of cell biology and are used as powerful probes to monitor an extensive array of entities, bioluminescence imaging is rapidly emerging as a new and quantitative approach to understanding cell physiology. We therefore verify whether bioluminescence imaging can be performed using C9-fused ELuc. As shown in Fig. 5c, A9 cells carrying a cassette consisting of NF-κB response element, TK promoter, and C9-fused ELuc on the MI-HAC vector were transiently treated with TNFα for 15 min. CCD images were captured for 10 min at 15-min intervals for 15 h using a luminescence microscope, and light intensities from 25 cells were quantified. As shown in Fig. 6, after treatment with TNFα, the luminescence intensities rapidly increased, reached a maximum, and subsequently decreased, and this tendency was similar to what was observed in the photomultiplier recordings shown in Fig. 5c. The peak times of the 25 quantified cells varied from 3 to 8 h, which might be due to differences in sensitivity to TNFα of the cells. Thus, we were able to clearly capture and quantify acute gene expression in a cell by means of time-lapse bioluminescence imaging with C9-fused ELuc.

4. Discussion

We have identified a destabilization sequence consisting of 42 amino acid residues from the C9 fragment of hCAPN3 (Fig. 2b), and succeeded in destabilizing two luciferases, ELuc and *luc2*, in the cells by fusing the C9 fragment (Figs. 2a and 4a). Moreover, we have demonstrated that a highly sensitive luciferase reporter assay could be achieved by using C9-fused ELuc rather than PEST-fused ELuc, in which acute gene expression was tracked by means of real-time bioluminescence recording and single-cell bioluminescence imaging (Figs. 5c and 6). Although the light intensity of C9-fused ELuc was reduced to less than 1% of the light intensity of unmodified ELuc, the light intensity is enough to produce reliable results, and the speed and magnitude of the activation kinetics of NF-κB could be monitored with high sensitivity using the C9-fused ELuc.

The PEST sequence from ornithine decarboxylase is widely used to reduce the stability of reporter gene in cells. Previous studies have demonstrated that the degradation rate of firefly luciferase, the most typical beetle luciferase reporter gene, is increased by 3–4-fold by fusing PEST in T-47D cells (Leclerc et al., 2000) and HeLa cells (Voon et al., 2005), being consistent with our study in which measurements were carried out in NIH3T3 (Fig. 2) and A9 (Fig. S6b) cells using ELuc. An even more rapid destabilization of firefly luciferase was accomplished by the combined use of PEST and RNA degradation signal, which resulted in an approximately 6-fold higher degradation rate than that of wild-type luciferase in HeLa cells (Voon et al., 2005). As shown in Figs. 2a and S6b, the degradation rates of ELuc fused to the C9 fragment were 10- and

14-fold of that of unmodified ELuc in NIH3T3 and A9 cells, respectively. Although we cannot make a direct comparison because the luciferases, cells, and measurement systems used were not identical between this study and previous studies, it may be reasonable to assume that the C9 fragment is a much more potent destabilization sequence that reduces the stability of luciferase in the cells than the combination of PEST and RNA degradation signal.

Western blot analysis demonstrated that C9-fused ELuc is rapidly reduced in cells in the presence of the protein synthesis inhibitor cycloheximide (Fig. 3a), indicating that the loss of luminescence intensity by fusing the C9 fragment is due not to interference with the luciferin-luciferase reaction, but to the acceleration of the proteolytic degradation of luciferase in the cells. CAPN3, which has four domains, is a calcium- or sodium-dependent cysteine protease, and its half-life is very short due to autoproteolytic degradation (Sorimachi et al., 2011). In this study, the identified C9 fragment is a partial sequence of domain III. Domain II, or the so-called autolytic activation domain, plays a role in the autoproteolysis of CAPN3, whereas domain III, or the so-called C2-like domain, participates in the binding of calcium and phospholipid. Both are required for promoting calpain activation, but are not directly involved in autolysis (Duguez et al., 2006). Thus, even though the C9 fragment dramatically reduces the stability of luciferase, further study is needed to elucidate the mechanism of the induction of the rapid degradation of luciferase in the cells by fusing the C9 fragment.

To verify the effects of PEST and C9 fragment on the sensitivity of the luciferase reporter assay, we used stable A9 cells harboring the MI-HAC vector, in which a reporter plasmid was inserted into the target site of the vector. Although the transient transfection of reporter gene is conventionally used to introduce a reporter gene into the host cells and to monitor cellular response, heterogeneities in the transfection efficiency and the plasmid copy number among the transfected cells sometimes result in differences in the amount of expressed reporter protein, and consequently differences in cellular response measured by the reporter. Even though stable cell lines can be generated by the conventional method in which a reporter gene is randomly integrated into the chromosome of host cells, it is impossible to avoid the positional effect and to regulate the copy number of the reporter gene. To resolve these issues, we inserted a reporter plasmid into a specific site of the MI-HAC vector, where both copy number and integration site of the reporter plasmid could be accurately regulated. By doing so, the responsiveness of cells monitored by luciferases having different stabilities in the cells could be precisely compared. Thus, the MI-HAC vector is useful not only for carrying transgene as a reporter vector but also for evaluating the characteristic properties of luciferase in the cells.

We also found that the C9 fragment destabilized EGFP after its fusion to the C-terminus of EGFP in NIH3T3 cells, as demonstrated by immunoblot analysis using anti-EGFP antibody (Fig. 4b). Together, the results demonstrate that the C9 fragment is broadly applicable to not only the luciferase reporter assay, including real-time recording and bioluminescence imaging, but also fluorescence imaging. Thus, the destabilization sequence identified in this study should be useful for a broad range of sensitive reporter assays that require measurement of acute response kinetics in the cells, including cell-based and cell-chip assays.

Disclosure statement

Patent registration for this work is under way.

Acknowledgments

We thank S. Kumata, M. Kondo, S. Sasaguri N. Ueda, and T. Iwaki of AIST for excellent technical assistance. This study was supported in part by the New Energy and Industrial Technology Development (NEDO), Japan (No. P06040), and by ARCH-Tox project from the Ministry of Economy, Trade and Industry (METI), Japan.

Appendix A. Supplementary data

Supplementary data associated with this article can be found, in the online version, at http://dx.doi.org/10.1016/j.jbiotec.2014.12.004.

References

Duguez, S., Bartoli, M., Richard, I., 2006. Calpain 3: a key regulator of the sarcomere? FEBS J. 273, 3427–3436.

Fanin, M., Nascimbeni, A.C., Angelini, C., 2007. Screening of calpain-3 autolytic activity in LGMD muscle: a functional map of CAPN3 gene mutations. J. Med. Genet. 44, 38–43.

Greer 3rd, L.F., Szalay, A.A., 2002. Imaging of light emission from the expression of luciferases in living cells and organisms: a review. Luminescence 17, 43–74.

Gross, S., Piwnica-Worms, D., 2005. Spying on cancer: molecular imaging *in vivo* with genetically encoded reporters. Cancer Cell 7, 5–15.

Grygorczyk, R., Furuya, K., Sokabe, M., 2013. Imaging and characterization of stretch-induced ATP release from alveolar A549 cells. J. Physiol. 591, 1195–1215.

Katoh, M., Ayabe, F., Norikane, S., Okada, T., Masumoto, H., Horike, S., Shirayoshi, Y., Oshimura, M., 2004. Construction of a novel human artificial chromosome vector for gene delivery. Biochem. Biophys. Res. Commun. 321, 280–290.

Kazuki, Y., Hoshiya, H., Takiguchi, M., Abe, S., Iida, Y., Osaki, M., Katoh, M., Hiratsuka, M., Shirayoshi, Y., Hiramatsu, K., Ueno, E., Kajitani, N., Yoshino, T., Kazuki, K., Ishihara, C., Takehara, S., Tsuji, S., Ejima, F., Toyoda, A., Sakaki, Y., Larionov, V., Kouprina, N., Oshimura, M., 2011. Refined human artificial chromosome vectors for gene therapy and animal transgenesis. Gene Ther. 18, 384–393.

Kwon, H.J., Ohmiya, Y., Yasuda, K., 2012. Dual-color system for simultaneously monitoring intracellular Ca^{2+} and ATP dynamics. Anal. Biochem. 430, 45–47.

Leclerc, G.M., Boockfor, F.R., Faught, W.J., Frawley, L.S., 2000. Development of a destabilized firefly luciferase enzyme for measurement of gene expression. BioTechniques 29, 594–596.

Luker, K.E., Luker, G.D., 2008. Applications of bioluminescence imaging to antiviral research and therapy: multiple luciferase enzymes and quantitation. Antiviral Res. 78, 179–187.

Ling, J., Kumar, R., 2012. Crosstalk between NFκB and glucocorticoid signaling: a potential target of breast cancer therapy. Cancer Lett. 322, 119–126.

Nakajima, Y., Ohmiya, Y., 2010. Bioluminescence assays: multicolor luciferase assay, secreted luciferase assay and imaging luciferase assay. Expert Opin. Drug Discov. 5, 835–849.

Nakajima, Y., Yamazaki, T., Nishii, S., Noguchi, T., Hoshino, H., Niwa, K., Viviani, V.R., Ohmiya, Y., 2010. Enhanced beetle luciferase for high-resolution bioluminescence imaging. PLoS One 5, e10011.

Naylor, L.H., 1999. Reporter gene technology: the future looks bright. Biochem. Pharmacol. 58, 749–757.

Rechsteiner, M., Rogers, S.W., 1996. PEST sequences and regulation by proteolysis. Trends Biochem. Sci. 21, 267–271.

Roda, A., Guardigli, M., Michelini, E., Mirasoli, M., 2009. Bioluminescence in analytical chemistry and *in vivo* imaging. Trends Anal. Chem. 28, 307–322.

Sorimachi, H., Hata, S., Ono, Y., 2011. Impact of genetic insights into calpain biology. J. Biochem. 150, 23–37.

Sorimachi, H., Toyama-Sorimachi, N., Saido, T.C., Kawasaki, H., Sugita, H., Miyasaka, M., Arahata, K., Ishiura, S., Suzuki, K., 1993. Muscle-specific calpain, p94, is degraded by autolysis immediately after translation, resulting in disappearance from muscle. J. Biol. Chem. 268, 10593–10605.

Tomizuka, K., Yoshida, H., Uejima, H., Kugoh, H., Sato, K., Ohguma, A., Hayasaka, M., Hanaoka, K., Oshimura, M., Ishida, I., 1997. Functional expression and germline transmission of a human chromosome fragment in chimaeric mice. Nat. Genet. 16, 133–143.

Tornatore, L., Thotakura, A.K., Bennett, J., Moretti, M., Franzoso, G., 2012. The nuclear factor kappa B signaling pathway: integrating metabolism with inflammation. Trends Cell Biol. 22, 557–566.

Voon, D.C., Subrata, L.S., Baltic, S., Leu, M.P., Whiteway, J.M., Wong, A., Knight, S.A., Christiansen, F.T., Daly, J.M., 2005. Use of mRNA- and protein-destabilizing elements to develop a highly responsive reporter system. Nucleic Acids Res. 33, e27.

Welsh, D.K., Kay, S.A., 2005. Bioluminescence imaging in living organisms. Curr. Opin. Biotechnol. 16, 73–78.

Welsh, D.K., Takahashi, J.S., Kay, S.A., 2010. Suprachiasmatic nucleus: cell autonomy and network properties. Annu. Rev. Physiol. 72, 551–577.

Wilson, T., Hastings, J.W., 1998. Bioluminescence. Annu. Rev. Cell Dev. Biol. 14, 197–230.

Yamaguchi, S., Kazuki, Y., Nakayama, Y., Nanba, E., Oshimura, M., Ohbayashi, T., 2011. A method for producing transgenic cells using a multi-integrase system on a human artificial chromosome vector. PLoS One 6, e17267.